Shunt Active Power Control Based on Feed-Forward Neural Network

Gideon F. Tano-Boamah
Dept. of Electrical/Electronic Engineering
Kwame Nkrumah University of Science and Technology
Kumasi, Ghana

***Abstract*—The shunt active power filter (SAPF) represents a prevalent instrument for the mitigation of harmonic distortions in three-phase electrical power systems. Numerous control methodologies have been established, encompassing approaches grounded in Artificial Neural Networks. Nevertheless, the conventional feedforward neural network, which has demonstrated efficacy in addressing various nonlinear challenges, has yet to be utilized with optimal performance in the execution of the SAPF control aimed at producing the reference currents for three-phase inverters. To validate the potential of this straightforward neural architecture, this study delineates an appropriate application strategy, predicated on the precise estimation of the Fourier coefficients associated with the fundamental harmonic of any distorted voltage or current. The aims included harmonic reduction and enhancement of the power factor. By utilizing simulations and experimental design, I evaluated practical scenarios, thereby confirming the feasibility of the recommended strategy.**

***Index Terms*—feed-forward neural network, harmonics compensation, shunt active power filter, frequency, power quality, total harmonic distortion, power factor**

I. Introduction

Power systems, particularly distribution networks, are facing significant challenges related to power quality in the current era of advanced power electronics [11], [16], [26]. The expansion of power electronics-based nonlinear loads is causing harmonics within distribution systems. The widespread deployment of such nonlinear equipment has escalated the need for harmonics mitigation and reactive power compensation [27].

The adverse effects of poor power quality, resulting from the presence of harmonics and distortions, include power loss, resonance, overheating, and failures of power protection devices and electrical and electronic equipment. These issues impose substantial costs on both consumers and utility providers [9], [18], [28]. Addressing power quality concerns necessitates dedicated attention and extensive efforts for improvement. Harmonics generated by nonlinear loads induce voltage distortion, adversely affecting other connected loads at the same point of common coupling.

Researchers over the years have proposed various methods for mitigating the harmonics in the power system. Initially, capacitor banks were suggested as a solution which were found to be ineffective in periods of overvoltage. Also, the issue of resonance arises when the reactance offered by the capacitor bank becomes equal to the system inductive reactance [29]. In that event, filters were developed to address harmonics and reactive power issues in power systems.

Several traditional methods including Instantaneous Active Power and Reactive Power Theory, and Synchronous Reference Frame Theory have been used in controlling the SAPF to detect and mitigate harmonics. The traditional methods employ the use of filters which limit their ability to handle non-linear and time-varying characteristics of the system. Other traditional methods used in SAPF that are PI controllers and Repetitive controllers perform poorly in unbalanced and non-ideal cases. The advent of machine learning techniques has brought new opportunities for controlling SAPFs resulting in more efficient and accurate power quality enhancement [12], [18], [21].

Artificial Intelligence (AI) based control methods such as Artificial Neural Networks have shown great potential in enhancing the performance of SAPFs and can learn from system behavior and adapt to changing operating conditions which traditional techniques cannot do. The AI based technique control can improve the accuracy and speed of the system and can handle complex non-linear systems.

In retrospect of the ongoing research in the application of AI techniques in controlling the Shunt Active Power Filter, we aim to design a SAPF controller based on AI techniques.

II. Method of Compensation

The Fourier Transform is a mathematical operation that transforms a time-domain function $f(t)$ into a frequency-domain representation $F(\omega)$, where ω represents angular frequency.

This transformation expresses the original function as a sum of sinusoids with varying amplitudes and phases. With the frequency domain analysis, signals are decomposed as the sum of fundamental $\sin \omega t$ and $\cos \omega t$ with harmonics.

$$F(\omega) = \int_{-\infty}^{\infty} f(t) e^{-i\omega t}\, dt \tag{1}$$

where $F(\omega)$ is the Fourier Transform of $f(t)$.

However, three-phase quantities are periodic due to their sinusoidal nature. The transformation of continuous periodic signals leads to the formation of the Fourier Series.

The neural network is the control system of the proposed shunt active power filter. For the neural network to actively provide accurate reference current for the power converter, the data of the system must be fed to the control block. Because the voltage and current of a three-phase system are continuous time signals, there is a need to convert these waveforms into discrete waveforms. Sampling is done by multiplying the continuous signal by a delta function or an impulse train. The neural networks are designed to process discrete signals. Fourier transforms are used in the generation of reference current. The computation of Fourier transforms of continuous signals is complex. Sampling produces periodic and finite signals [1].

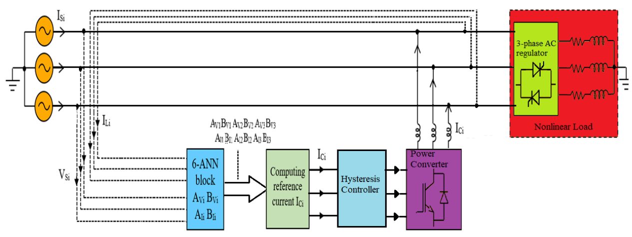

Fig. 1. A general overview of the proposed system into the transformer-less grid.

The distorted current waveform can be described as the combination of various sinusoidal components, each with frequencies that are multiples of a base frequency [1].

$$I_{L,i}(t) = \sqrt{2}\, I_{1,i} \cos(\omega t - \varphi_{1,i}) + \sqrt{2} \sum_{\forall h \geq 2} I_{h,i} \cos(h\omega t - \varphi_{h,i}) \tag{2}$$

$$I_{C,i}(t) = I_{L,i}(t) - I_{S,i}(t) = \sqrt{2} \sum_{\forall h \geq 2} I_{h,i} \cos(h\omega t - \varphi_{h,i}) \tag{3}$$

The source current obtained after compensation is

$$I_{S,i}(t) = \sqrt{2}\, I_{1,i} \cos(\omega t - \varphi_{1,i}) \tag{4}$$

which is expressed through their rectangular components as

$$\begin{aligned} I_{S,i}(t) &= \sqrt{2}\, I_{1,i} \cos(\omega t - \varphi_{1,i}) \\ &= \sqrt{2}\, I_{1,i} \cos\varphi_{1,i} \cos\omega t + \sqrt{2}\, I_{1,i} \sin\varphi_{1,i} \sin\omega t \\ &= A_{I,i} \cos\omega t + B_{I,i} \sin\omega t \end{aligned} \tag{5}$$

where $A_{I,i}$ and $B_{I,i}$ are real numbers representing the rectangular coefficients of the fundamental source current. This implies the compensation current obtained is expressed as

$$I_{C,i}(t) = I_{L,i}(t) - (A_{I,i} \cos\omega t + B_{I,i} \sin\omega t) \tag{6}$$

The expressions for the compensating currents of the three phases are:

$$I_{C,a}(t) = I_{L,a}(t) - (A_{I,i} \cos\omega t + B_{I,i} \sin\omega t) \tag{7}$$

$$\begin{aligned} I_{C,b}(t) = I_{L,b}(t) - \Big(& A_{I,i} \cos\Big(\omega t + \frac{2\pi}{3}\Big) \\ & + B_{I,i} \sin\Big(\omega t + \frac{2\pi}{3}\Big)\Big) \end{aligned} \tag{8}$$

$$\begin{aligned} I_{C,c}(t) = I_{L,c}(t) - \Big(& A_{I,i} \cos\Big(\omega t - \frac{2\pi}{3}\Big) \\ & + B_{I,i} \sin\Big(\omega t - \frac{2\pi}{3}\Big)\Big) \end{aligned} \tag{9}$$

III. Power Factor Compensation

The APF is designed to inject currents aimed at reducing harmonic distortion and correcting the power factor. Power factor correction is achieved when the source current, following compensation, aligns closely with the voltage phase. To ensure this alignment, a corrective factor derived from the phase voltages is used. These corrective factors help adjust the compensation currents so that the phase currents are nearly in phase with the voltages. This correction is essential because current distortion leads to corresponding voltage distortion [1].

$$I_{S,i}(t) = G\, V_{S,x}(t) \tag{10}$$

where G is the corrective factor or equivalent conductance,

$$G = \frac{P}{V^2} = \frac{P}{V_a^2 + V_b^2 + V_c^2} \tag{11}$$

P represents the average power used by the load, while V is the RMS value of the three-phase voltage, calculated from the RMS values of the phase voltages. The phase voltages are displaced by 120° from each other, and the source voltage is

$$V_{S,x}(t) = \sqrt{2}\, V_{S,x} \cos(\omega t + \alpha) \tag{12}$$

where α is the displacement angle.

The FFNN could also generate a rectangular coefficient of the voltage as:

$$V_{C,a}(t) = V_{L,a}(t) - (A_{V,a} \cos\omega t + B_{V,a} \sin\omega t) \tag{13}$$

$$\begin{aligned} V_{C,b}(t) = V_{L,b}(t) - \Big(& A_{V,b} \cos\Big(\omega t + \frac{2\pi}{3}\Big) \\ & + B_{V,b} \sin\Big(\omega t + \frac{2\pi}{3}\Big)\Big) \end{aligned} \tag{14}$$

$$\begin{aligned} V_{C,c}(t) = V_{L,c}(t) - \Big(& A_{V,c} \cos\Big(\omega t - \frac{2\pi}{3}\Big) \\ & + B_{V,c} \sin\Big(\omega t - \frac{2\pi}{3}\Big)\Big) \end{aligned} \tag{15}$$

$$\begin{aligned} P_i(t) &= V_i(t) \cdot I_i(t) \\ &= (A_{V,i} \cos\omega t + B_{V,i} \sin\omega t)(A_{I,i} \cos\omega t + B_{I,i} \sin\omega t) \end{aligned} \tag{16}$$

for $i = a, b, c$. The application of trigonometric identities in (16) allows us to obtain

$$P_i(t) = \frac{A_{V,i}A_{I,i} + A_{V,i}B_{I,i} + B_{V,i}A_{I,i}}{2} \sin 2\omega t \\ +(B_{V,i}B_{I,i} - A_{V,i}A_{I,i}) \sin 2\omega t \tag{17}$$

The active power for phase i is the average value of $P_i(t)$ over a period:

$$P_i = \frac{1}{T}\int_0^T P_i(t)\,dt = \frac{A_{V,i}A_{I,i} + B_{V,i}B_{I,i}}{2} \tag{18}$$

In a three-phase system, the calculation of the three active powers of each phase determines the total active power:

$$P_i = \frac{1}{2}(A_{V,a}A_{I,a} + B_{V,a}B_{I,a} + A_{V,b}A_{I,b} \\ +B_{V,b}B_{I,b} + A_{V,c}A_{I,c} + B_{V,c}B_{I,c}) \tag{19}$$

The RMS value of the three-phase voltage as a function of rectangular coefficients is

$$V^2 = V_a^2 + V_b^2 + V_c^2 \tag{20}$$

where for each phase it is verified that

$$\sqrt{2}\,V_i = \sqrt{A_{Vi}^2 + B_{Vi}^2} \tag{21}$$

and therefore

$$V^2 = \frac{1}{2}(A_{Va}^2 + B_{Va}^2 + A_{Vb}^2 + B_{Vb}^2 + A_{Vc}^2 + B_{Vc}^2) \tag{22}$$

From (19) and (22), G is obtained as:

$$G = \frac{A_{Va}A_{Ia} + B_{Va}B_{Ia} + A_{Vb}A_{Ib} + B_{Vb}B_{Ib} + A_{Vc}A_{Ic} + B_{Vc}B_{Ic}}{A_{Va}^2 + B_{Va}^2 + A_{Vb}^2 + B_{Vb}^2 + A_{Vc}^2 + B_{Vc}^2} \tag{23}$$

The conductance equivalence factor G expressed in simple terms of the rectangular coefficients is:

$$G = \frac{A_V A_I + B_V B_I}{A_V^2 + B_V^2} \tag{24}$$

$$I_{C,i}(t) = I_{L,i}(t) - G\,V_{S,i} \tag{25}$$

$$I_{C,a}(t) = I_{L,a}(t) - G(A_V \cos\omega t + B_V \sin\omega t) \tag{26}$$

$$I_{C,b}(t) = I_{L,b}(t) - G\Big(A_V \cos\left(\omega t - \frac{2\pi}{3}\right) \\ +B_V \sin\left(\omega t - \frac{2\pi}{3}\right)\Big) \tag{27}$$

$$I_{C,c}(t) = I_{L,c}(t) - G\Big(A_V \cos\left(\omega t + \frac{2\pi}{3}\right) \\ +B_V \sin\left(\omega t + \frac{2\pi}{3}\right)\Big) \tag{28}$$

The Fourier coefficients are used to reconstruct the source current into continuous form using:

$$a_0 + \sum_{n=1}^{\infty}\left(a_n \cos\left(\frac{2\pi n x}{T}\right) + b_n \sin\left(\frac{2\pi n x}{T}\right)\right) \tag{29}$$

IV. Artificial Neural Network

The feed-forward neural network consists of a determined number of neurons, organized in two or more layers, highly interconnected. The neuron operation consists of applying a determined transfer function to a weighted sum of its inputs. It is usual to choose a "tan-sigmoid" transfer function for hidden layers and a "linear" function for the output layer. The performance index, MSE, measures the accuracy of the neural network [1].

$$mse = \frac{1}{m}\sum_{i=1}^{m}\|y - t\|^2 \tag{30}$$

where m is the number of training patterns and y and t correspond to the output and target vectors respectively. The backpropagation algorithm uses the mean square error to re-adjust the interconnection weights to reduce the mean square error. This cycle is iteratively repeated until the mean square error reaches a small enough value.

In this project, different backpropagation training algorithms were used, such as Bayesian Regularization, Scaled Conjugate Gradient, Resilient Backpropagation, and the Levenberg–Marquardt algorithm. Among these, the Levenberg–Marquardt algorithm gave the best mean square error, 6.7×10^{-6}, with the fewest number of epochs, about 11. The resilient backpropagation algorithm provided a similar mean square error but required more epochs, about 35.

After extensive tests with different numbers of points per cycle and FFNN inputs, a sampling rate of 5 kHz was chosen, with 30 points per waveform cycle, meaning the neural network must contain 30 inputs. For the strategy of extracting the fundamental harmonic, there was no need to increase the number of samples. It also works with faster sampling, but at the cost of increasing the size and complexity of the FFNN, as well as the training time, without achieving higher performance.

Different harmonic spectra of nonlinear loads were analyzed to choose suitable magnitudes for the different harmonics. The control approach for the shunt active filter involves sampling each waveform cycle of current or voltage to provide the input for the artificial neural network. The method was initially tested at a standard 50 Hz frequency, and the model was designed to function effectively across a range of frequencies. For the 50 Hz case, the ANN provides rectangular coefficients for the fundamental harmonic every 20 milliseconds.

It is important for the control method to perform optimally even with variations from the standard 50 Hz, to ensure model stability. The training data included multiple waveforms with frequencies close to the fundamental frequency, incorporating frequencies varying between 49.5 Hz and 50.5 Hz [1].

A voltage source inverter was used as the power conversion stage within the framework of the SAPF. The inverter facilitates the transformation of direct current (DC) voltage obtained from the DC link capacitor into alternating current (AC) outputs, which are subsequently integrated into the electrical power system. The DC link capacitor serves as the voltage source essential for the functionality of the inverter [8], [9], [15], [25].

An insulated-gate bipolar transistor (IGBT)-based inverter is proposed because IGBTs combine the advantages of the MOSFET and BJT. The IGBTs act as switches in the inverter circuit, and the gating signals for the IGBTs are generated by a current control technique.

V. Simulation

This project was simulated in the MATLAB/Simulink environment. It demonstrated the application of artificial intelligence methods to control a shunt active power filter to mitigate harmonics generated by non-linear loads. The system parameters are given in Table I.

TABLE I
System Parameters Used in the Simulation

Parameter	Value
AC Source Voltage	415 V
System Frequency	50 Hz
Total line impedance per line	$R_s = 0.012\,\Omega$, $L_s = 0.0625$ mH
Sampling Frequency	5000 Hz
Hysteresis controller	Hysteresis band ± 0.07
Shunt Active Power Filter	
Filter Impedance	$L_s = 4.06$ mH
DC Link Capacitor Voltage	415 V
DC Link Capacitor Capacitance	4700 μF
Load	
Resistance	20 Ω
Inductance	90 mH

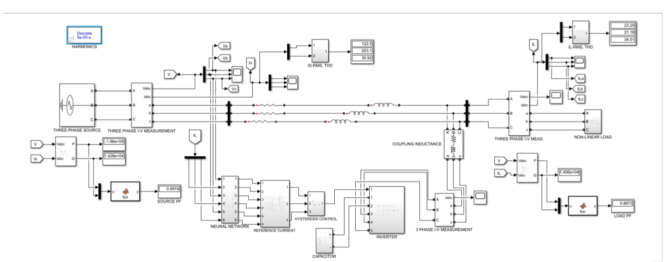

Fig. 2. Simulation of the proposed system in MATLAB.

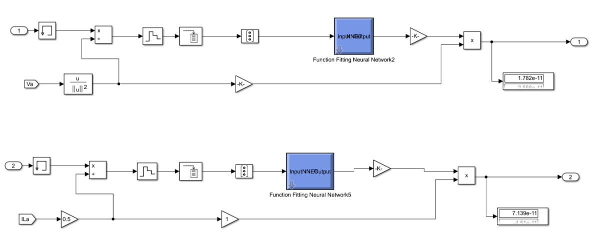

Fig. 3. An illustration of the neural network controller of the SAPF.

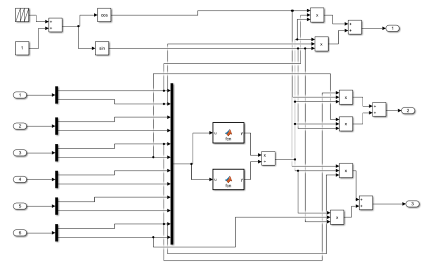

Fig. 4. An illustration of the calculation of the source current.

VI. Results and Analysis

This section presents the findings from the simulations along with a comprehensive analysis of the results. The main aim of minimizing harmonic distortion was evaluated by measuring the Total Harmonic Distortion (THD) of the system, with a target of achieving values below 5%. Additionally, the unity power factor compensation control method aims to attain a power factor close to one, alongside maintaining a low THD.

An unbalanced nonlinear load scenario arises when a diode bridge rectifier is linked to a three-phase unbalanced R-L load. The harmonic spectrum analysis for phase three, before any compensation, is presented in Fig. 5. The total harmonic distortion of the system is 54.02%, which exceeds IEEE standards.

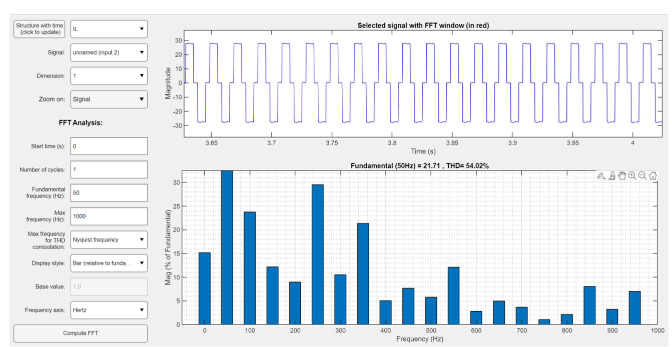

Fig. 5. Diagram of the THD of the load current before compensation.

With the connection of the feed-forward controlled SAPF into the system, it was observed that the sinusoidal wave was restored to some extent and a THD of 2.58% was obtained, which is safe under the IEEE standards. The power factor increased from 0.8673 to 0.9973.

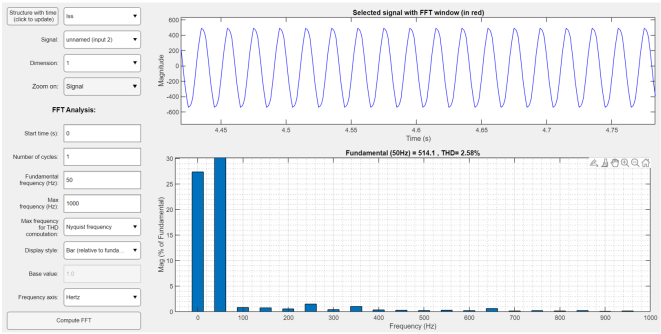

Fig. 6. Diagram of the THD of the source current after compensation.

A bridge impedance of $R = 10\,\Omega$ and $L = 70$ mH was connected to the nonlinear load. The THD of the system was found to be 33.03% with a power factor of 0.4927. The THD improved to 2.49% and the power factor increased to 0.8430.

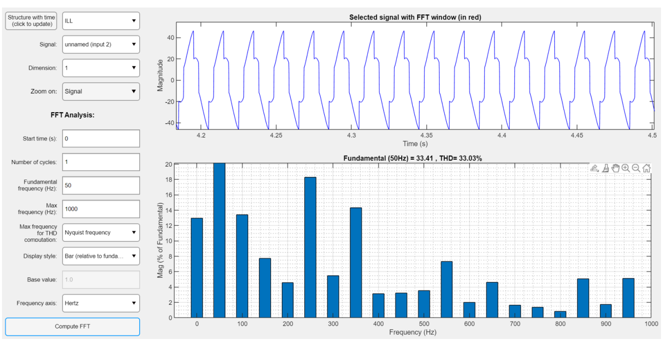

Fig. 7. Diagram of the THD with added bridge impedance.

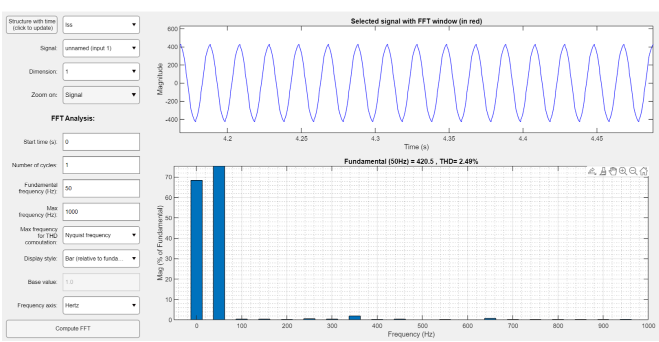

Fig. 8. Diagram of the THD after compensation with added bridge impedance.

Subsequent tests were performed on the system by varying the resistance, which showed that the load THD varied from 53% to 60% and the source THD from 2.43% to 2.51%. The frequency of practical systems is not a constant value but varies; standards regulate the allowable variation of frequency to ensure stability in the power system. The model was tested against the allowable frequency variation of $\pm 5\%$ of the nominal frequency, from 49.5 Hz to 50.5 Hz, with the results shown in Table II.

TABLE II
VARIATION OF THD WITH FREQUENCY

Frequency (Hz)	**Load THD (%)**	**Source THD (%)**
49.50	34.56	2.79
49.70	33.79	2.56
50.10	32.65	2.51
50.30	32.27	2.51
50.50	31.51	2.57

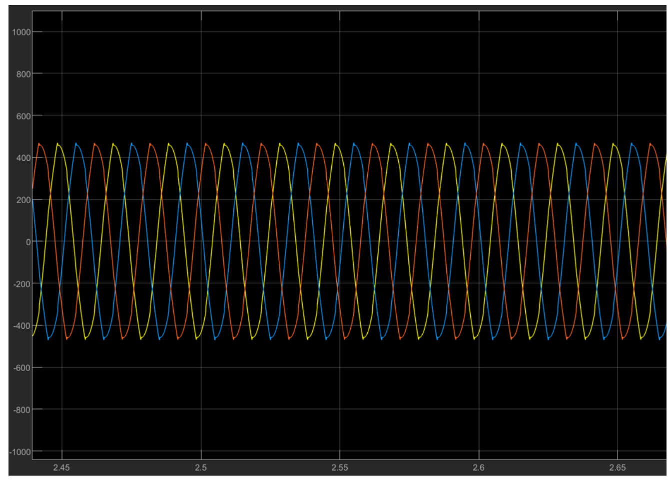

Fig. 9. Illustration of the source current waveform.

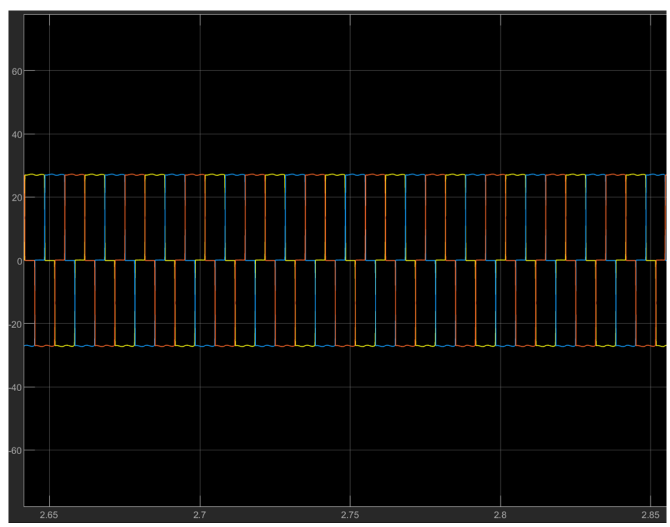

Fig. 10. Illustration of the load current waveform.

VII. Conclusion

Feedforward Neural Network integration with shunt active power filters provides a dynamic and innovative solution to improve power quality in modern electrical systems. The project work established the implications of using a Feedforward Neural Network Controlled SAPF as a potent instrument to address power quality issues, with an emphasis on its realistic application using MATLAB/Simulink simulation.

References

[1] J. L. Flores-Garrido, P. S., and J. A. G.-G., "Nonlinear Loads Compensation Using a Shunt Active Power Filter Controlled by Feedforward Neural Networks," *Applied Sciences*, vol. 11, no. 16, Aug. 2021.

[2] M. Q. and V. Khadkikar, "Application of Artificial Neural Networks for Shunt Active Power Filter Control," *IEEE Transactions on Industrial Informatics*, vol. 10, pp. 1765–1774, 2014.

[3] S. and N. R. V. Jarupula, "Power Quality Improvement in Distribution System using ANN Based Shunt Active Power Filter," *International Journal of Power Electronics and Drive Systems*, vol. 5, pp. 568–575, 2015.

[4] G. S. G. and A. Joshi, "Artificial Neural Network Controlled Shunt Active Power Filter For Power Quality Improvement," *International Research Journal of Engineering and Technology (IRJET)*, vol. 2, no. 4, Jul. 2015.

[5] V. V. Pitchumani Angayarkanni, "A Neural Network Controller with Anti Windup Based Shunt Active Power Filter for Harmonic Mitigation," 2016.

[6] B. and M. P. M. Balasubramaniam, "Implementation of Artificial Neural Network Controlled Shunt Active Power Filter for Current Harmonics Compensation," *International Journal of Advanced Research in Computer and Communication Engineering*, vol. 4, no. 5, May 2015.

[7] S. M. I. C. and R. B. Abderrahmen Benyamina, "Hybrid fuzzy logic-artificial neural network controller for shunt active power filter," *IEEE International Conference on Renewable Energy Research and Applications (ICRERA)*, pp. 837–844, 2016.

[8] P. T. and R. T. D., "Adaptive Method for Power Quality Improvement through Minimization of Harmonics Using Artificial Intelligence," *International Journal of Power Electronics and Drive Systems (IJPEDS)*, vol. 8, no. 1, pp. 470–482, 2017.

[9] K. C. Patel, A. V. S., and M. H. G., "Shunt active filtering with NARX feedback neural networks based reference current generation," *International Conference on Power and Embedded Drive Control (ICPEDC)*, pp. 280–285, 2017.

[10] N. L. and J. Fei, "Adaptive Fractional Sliding Mode Control of Active Power Filter Based on Dual RBF Neural Networks," *IEEE Access*, vol. 5, pp. 27590–27598, Nov. 2017.

[11] S. Merabet, S. D. O. A., and J. M. L., "Direct neural method for harmonic currents estimation using adaptive linear element," *Electric Power Systems Research*, vol. 152, pp. 61–70, Nov. 2017.

[12] P. C. Tah, A. K. P., and B. P. P., "Shunt Active Filter Based on Radial Basis Function Neural Network and p-q Power Theory," *International Journal of Power Electronics and Drive Systems (IJPEDS)*, vol. 8, no. 2, pp. 667–676, 2017.

[13] M. A. and D. Joshi, "Analysis of Shunt Active Filter with ANN based Controller," *International Journal of Computer Applications*, vol. 182, Dec. 2018.

[14] H. W. and J. Fei, "Nonsingular Terminal Sliding Mode Control for Active Power Filter Using Recurrent Neural Network," *IEEE Access*, vol. 6, pp. 67819–67829, Oct. 2018.

[15] G. G. and G. P. Kumar, "Power quality improvement at nonlinear loads using transformer-less shunt active power filter with adaptive neural fuzzy interface system supervised PID controllers," *International Transactions on Electrical Energy Systems*, vol. 30, no. 3, May 2020.

[16] K. R. Sugavanam, M. S., R. J., and P. V. K., "Convolutional Neural Network-based harmonic mitigation technique for an adaptive shunt active power filter," *Automatika*, vol. 62, pp. 471–485, Oct. 2021.

[17] A. Govind, A. P., and P. K., "Performance Enhancement of Shunt Active Power Filter Application using Adaptive Neural Network," *Authorea*, Mar. 2021.

[18] S. F. A.-G. and R. M. Nelms, "Performance of a Shunt Active Power Filter for Unbalanced Conditions Using Only Current Measurements," *Energies*, vol. 14, no. 2, p. 397, Jan. 2021.

[19] P. P. and S. Wasti, "Peak Demand Management in Micro Hydro using Battery Bank," *Journal of Water, Energy and Environment*, vol. 22, no. 22, pp. 34–40, 2018.

[20] A. Ramadan, S. K. I. H., and A. M. A., "A Novel Intelligent ANFIS for the Dynamic Model of Photovoltaic Systems," *Mathematical Methods in Energy Economy*, vol. 10, no. 8, p. 1286, Apr. 2022.

[21] A. A. Imam, R. S. Kumar, and Y. A. Al-Turki, "Modeling and Simulation of a PI Controlled Shunt Active Power Filter for Power Quality Enhancement Based on P-Q Theory," *MDPI: Power Electronics*, vol. 9, no. 4, Apr. 2020.

[22] R. K. and V. Indragandhi, "Current control techniques of single phase shunt active power filter – a review," *IOP Conference Series: Materials Science and Engineering*, vol. 623, no. 1, p. 012007, Oct. 2019.

[23] S. J. K. A. Kongpan Areerak, "Harmonic Detection for Shunt Active Power Filter Using ADALINE Neural Network," 2021.

[24] M. N. Uddin and M. T. Amin, "Design and Simulation of Active Power Filter Based on Feed Forward Neural Network for Harmonic Detection and Elimination," 2020.

[25] K. L. Areerak and T. Narongrit, "Shunt Active Power Filter Design Using Genetic Algorithm Method," 2020.

[26] Hydro Ottawa, "Power Quality," 2024.

[27] M. N. D. D., N. Al-Mutawaly, and J. L., "From transmission to distribution networks – harmonic impacts on modern grid," 2015.

[28] M. Bhaskar, S. Ankit, K. Soumya, and J. Ogle, "Analyzing Distribution Transformer Degradation with Increased Power Electronic Loads," 2021.

[29] D. D. Relji, N. S. V. V. Vasi, and Dj. V. Oros, "Power factor correction and harmonics mitigation based on phase shifting approach," 2021.